Available online at www.sciencedirect.com
ScienceDirect
Journal of Organometallic Chemistry 692 (2007) 3351–3362
Journal of Organometallic Chemistry
www.elsevier.com/locate/jorganchem

Two electroactive ferrocenyl chalcones as original optical chemosensors for Ca^{2+} and Ba^{2+} cations in CH_3CN

Béatrice Delavaux-Nicot [a,*], Jérôme Maynadié [a], Dominique Lavabre [b], Suzanne Fery-Forgues [b]

[a] *Laboratoire de Chimie de Coordination du CNRS, UPR 8241, 205, route de Narbonne, F-31077, Toulouse cedex 04, France*
[b] *Laboratoire des Interactions Moléculaires et Réactivité Chimique et Photochimique, UMR 5623 du CNRS, Université Paul Sabatier, F-31062, Toulouse cedex 9, France*

Received 7 March 2007; received in revised form 29 March 2007; accepted 29 March 2007
Available online 7 April 2007

Abstract

The optical study of ferrocenyl ligands **1**–**2** is presented, and reveals several interesting points. Contrary to their monosubstituted counterparts, these ligands exhibit fluorescence properties in acetonitrile. They can detect calcium, and also barium, by four different techniques: NMR, electrochemistry, UV–Vis absorption spectroscopy and fluorimetry in the same solvent. Each ligand detects both salts in the same manner by UV–Vis absorption and by fluorimetry. The response depends on the nature of the N terminal groups of the ligand. In each case, the ligand–calcium interaction is complex and involves 3–5 species in equilibrium in solution. Their association constants have been determined by fitting the UV–Vis data. Remarkably, for **2** and the calcium salts, nearly the same set of association constants can be used to fit not only the UV–Vis data obtained with calcium triflate (in a restricted range of concentration) or with calcium perchlorate, but also the NMR data obtained with calcium triflate. Interestingly, these results strengthen the fact that, in this family of compounds, the azacrown derivatives are less sensitive to high calcium triflate concentrations than their simple N-alkyl homologues. It is noteworthy that the complex non-monotonous fluorescence behaviour of compounds **1** and **2** upon Ca^{2+} or Ba^{2+} addition is quite original for ferrocenyl chalcones. These ligands constitute scarce examples of multi-signalling fluorescent ferrocenyl chemosensors for Ca^{2+} and Ba^{2+} cations in CH_3CN.

Keywords: Chalcone; Ferrocene; Chemosensors; Ligand–cation interaction; Optical properties

1. Introduction

There is a growing interest in redox molecules featuring fluorescent unit(s), because they are expected to play a key role in the design of new multi-signalling ion sensors [1]. Among these molecules, ferrocenyl compounds are very attractive electrochemical sensors as they offer the possibility to modulate ion–receptor interaction according to their redox state. For example, electrostatic interactions can be switched off by the oxidation of ferrocene to ferricinium. The modulation or control of the photophysical properties of a fluorescent moiety incorporated in such a molecule has even been announced as a fascinating challenge for modern chemistry [2]. Following this idea, recently, the fluorescence intensity of a bistable dyad was reversibly modulated, depending on the oxidation state of ferrocene [3]. Thus, the research area concerning this class of compounds opens up new horizons for electronics and optical memory devices [4].

In other respects, despite the varied and interesting studies devoted to ferrocenyl chalcones, [5], these compounds had never been examined as ion chemosensors until the beginning of our work. As far as we are concerned, to get a new generation of original electrochemical and optical ferrocenyl ion chemosensors [6], we have designed a family of ferrocenyl compounds according to a ''three-

* Corresponding author. Tel.: +33 (0) 5 61 33 31 00; fax: +33 (0)5 61 55 30 03.
E-mail address: delavaux@lcc-toulouse.fr (B. Delavaux-Nicot).

0022-328X/$ - see front matter © 2007 Elsevier B.V. All rights reserved.
doi:10.1016/j.jorganchem.2007.03.044

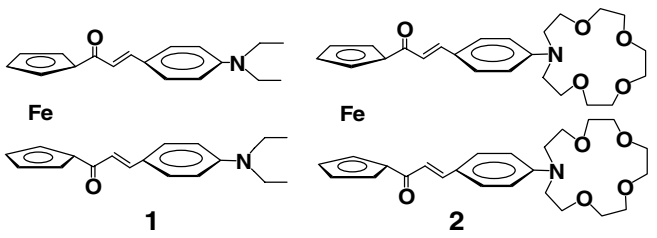

Scheme 1. Compounds **1** and **2**.

component conjugated system'' concept [6a,7]. In these compounds the ferrocenyl, complexing, and fluorescent moieties belong to the same conjugated electron system. In particular, we have showed that the monosubstituted ferrocenyl derivatives containing the basic fragment (—CO(CH=CH)C_6H_4-*p*-R), where R is an amino alkyl or azacrown group, are good electrochemical [8] and optical (UV–Vis absorption) [9] calcium sensors, though they are not fluorescent. However, the corresponding disubstituted compounds [Fe(C_5H_4CO(CH=CH)$_n$$C_6H_4$-*p*-R)$_2$], $n = 1$, R = NEt_2 (**1**) [6a] (Scheme 1), and $n = 2$, R = NMe_2 (**3**) display remarkable fluorescence properties in acetonitrile, and we have recently reported the capacity of **3** for behaving as a multi-responsive calcium chemosensor [7].

We are interested in the different factors that could influence cation detection in this family. Actually, numerous parameters such as the ligand framework, the nature of the salt (ion pair), as well as the medium or the detection method used have to be considered for the study of multi-signalling ion sensors. In particular, we have shown that an original electrochemical barium detection with regard to calcium detection was performed by compound **1** and its disubstituted azacrown counterpart [Fe(C_5H_4COCH=CHC_6H_4—*p*-aza-15-crown-5)$_2$] (**2**) (Scheme 1) [10], in contrast with their corresponding monosubstituted analogues [(C_5H_5)Fe(C_5H_4COCH=CHC_6H_4-*p*-NEt_2)] (**4**) and [(C_5H_5)Fe(C_5H_4COCH=CHC_6H_4-*p*-aza-15-crown-5)] (**5**). In this article, we focus on the capacity of compounds **1** and **2** for behaving as Ca^{2+} and Ba^{2+} optical chemosensors. Therefore, the UV–Vis absorption behaviour of these compounds in the presence of these cations is described and quantified. We show that each metal–ligand interaction gives rise to a complex equilibrium between several species in solution, and is representative of the nature of the ligand involved, this one being more or less sensitive to the experimental conditions employed. The uncommon and surprising fluorescence behaviour of compounds **1** and **2** upon addition of the two perchlorate salts is also presented.

2. Results and discussion

2.1. UV–Vis absorption study

2.1.1. Absorption characteristics of compounds 1 and 2

For comparison purpose, the absorption properties of these compounds were investigated in CH_3CN, as it was the case for the study of their NMR and electrochemical properties [10], and for the optical study of their monosubstituted counterparts [9].

As previously reported, the absorption spectrum of the monosubstituted compound [(C_5H_5)Fe(C_5H_4COCH=CHC_6H_4-*p*-NEt_2)] (**4**) (Fig. 1, bottom) displays two characteristic bands at 254 and 404 nm, a shoulder near 330 nm, and a long-wavelength absorption tail. The band at 254 nm can be attributed to a π–π^* transition characteristic of aromatic ketones, while the weak shoulder arises from a $n \rightarrow \pi^*$ transition [11]. The intense long-wavelength band was assigned to charge transfer (CT) occurring between the donor amino group and the acceptor carbonyl group. The broad low-intensity band located above 480 nm can be assigned to a d–d transition of iron in ferrocene [12]. The position of this band at long wavelengths can be explained by the electron acceptor effect of the organic moiety linked to ferrocene [12e].

The absorption spectra of the disubstituted compounds **1** and **2** studied in this work (Fig. 1, top) are rather similar in shape to that of monosubstituted compound **4**, and the same kind of band attribution can be done on the previous basis. As expected, the insertion of a second conjugated system in the molecular frame of **4** to give **1** induces a red shift of the maximum of the CT band from 404 to 414 nm, while the width of this band increases (full width at half-maximum = 3300 and 4300 cm^{-1} for **4** and **1**,

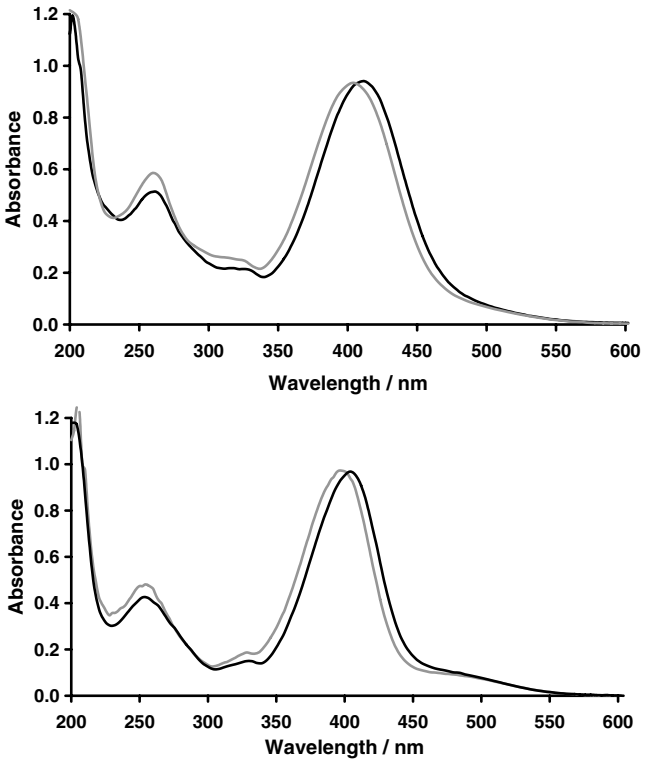

Fig. 1. Top: Absorption spectra of compounds **1** [2.1×10^{-5} M] (black line), and **2** [2.2×10^{-5} M] (grey line), in CH_3CN. Bottom: Absorption spectra of compounds **4** [2.9×10^{-5} M] (black line), and **5** [3.2×10^{-5} M] (grey line), in CH_3CN.

respectively). These results are in agreement with those obtained by Thomas et al. with polyferrocene compounds incorporating conjugated spacers [13]. The d–d transition is now partially overlapped because of the width of the CT band. As far as compound **2** is concerned, its absorption spectrum strongly resembles that of compound **1**, but the CT band is now slightly blue shifted by 10 nm. In this precise case, this phenomenon can be ascribed to the presence of the electron-withdrawing effect of the oxygen atoms in the crown ring, thus decreasing the donating character of the nitrogen atom [8,10]. A similar blue shift has also been observed when comparing the UV–Vis absorption spectrum of **4** with that of its azacrown counterpart [$(C_5H_5)Fe(C_5H_4COCH{=}CHC_6H_4$-*p*-aza-15-crown-5)] (**5**) [9], and with related organic compounds [14b]. However, this phenomenon is not systematically observed when substituting an amino alkyl group by an azacrown group in dye molecules [15].

2.1.2. Detection of calcium triflate by compounds *1* and *2*

Calcium triflate was employed in our previous work to study the electrochemical and NMR behaviour of compounds **1** and **2** in the presence of ions. We went on working with this salt for absorption study, so that the results obtained using different detection techniques were comparable. Our aim was to explore a wide range of concentration in calcium, which means that a high metal-to-ligand ratio should be attained.

Addition of calcium triflate to a solution of dye **1** (1.25×10^{-5} M) induced drastic changes in its absorption spectrum, and preliminary results have been published about this point [16b]. A two-step behaviour was typically observed: First, the intensity of the CT band slightly increased until 1 equiv. of salt was added. Then, it slowly decreased upon subsequent addition of salt (until a 3.0×10^{-3} M salt concentration) while λ_{max} shifted from 414 to 422 nm. A reddening of the solution was noted, corresponding to an increase of absorbance around 500 nm. This phenomenon was assigned to the interaction of the carbonyl group with the cation [16]. It should be noticed that no isosbestic points were observed, indicating that more than one equilibrium between **1** and the calcium cation was involved in solution.

Actually, complementary experiments showed that increasing further the salt concentration (until a 10^{-2} M salt concentration) induced a drastic decrease of the absorbance intensity at long wavelengths (after 400 nm), and the growth of a new band around 320 nm. This constitutes a new and final third step due to addition of calcium triflate.

For compound **2** (1.37×10^{-5} M), the absorption spectrum also varies strongly in the presence of calcium triflate. As noted for **1**, the intensity of the CT band first increases slightly. Then it decreases regularly, accompanied by a weak red-shift of the band. A new band appears at 332 nm, with the formation of two quasi-isosbestic points at 364 and 282 nm (Fig. 2, top). For calcium triflate concentration higher than 2.5×10^{-3} M (Fig. 2, bottom), the absorbance of the whole spectrum decreases, until a new band forms around 300 nm when the salt concentration reaches 3.0×10^{-2} M.

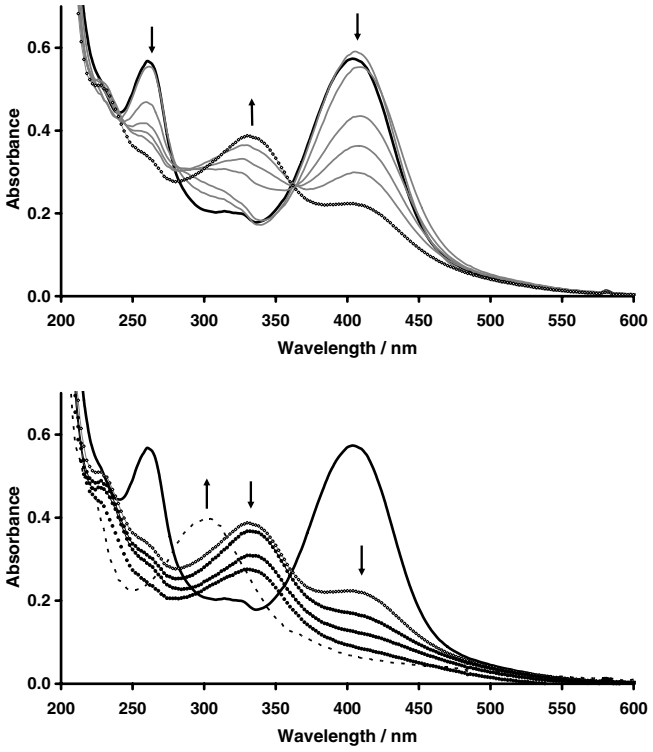

Fig. 2. Absorption behaviour of compound **2** [1.37×10^{-5} M] (solid line) upon calcium triflate addition, in CH_3CN. Top, from top to bottom, [Ca^{2+}] (M): 1.0×10^{-5}, 0.0, 5.0×10^{-5}, 2.5×10^{-4}, 5.0×10^{-4}, 1.0×10^{-3}, 2.5×10^{-3}; Bottom, from top to bottom, [Ca^{2+}] (M): 0.0, 2.5×10^{-3}, 5.0×10^{-3}, 7.5×10^{-3}, 1.0×10^{-2}, 3.0×10^{-2}.

Thus, for both ligands, the same main trends (disparition of the CT band and appearance of a new band around 300 nm) were characteristic features observed at high calcium triflate concentration (>2.5×10^{-3} M) and were more clearly observed for **2**.

Remembering the outcome of the results obtained with the monosubstituted compounds of this family under the same conditions, a protonation reaction was suspected to occur in this final step. Therefore, the UV–Vis behaviour of compounds **1** and **2** towards protonation was examined.

2.1.3. In situ protonation of compounds *1* and *2*

We have previously shown elsewhere that adding HBF_4 to solutions of compounds **1**–**2** effectively leads to their N-protonated homologues [10]. We investigated here the absorption behaviour of these compounds upon H^+ addition. Triflic acid was added stepwise to a solution of each compound in the 10^{-5} M range in CH_3CN. The solution turned clear (orange to very clear pink) and strong modifications of the spectrum were observed (Fig. 3). The intensity of the CT band (near 400 nm) progressively decreased while a new band appeared around 310 nm. Isosbestic points were formed, located at 348 nm for compound **1** and at 232, 266 and 348 nm for **2**. This behaviour is char-

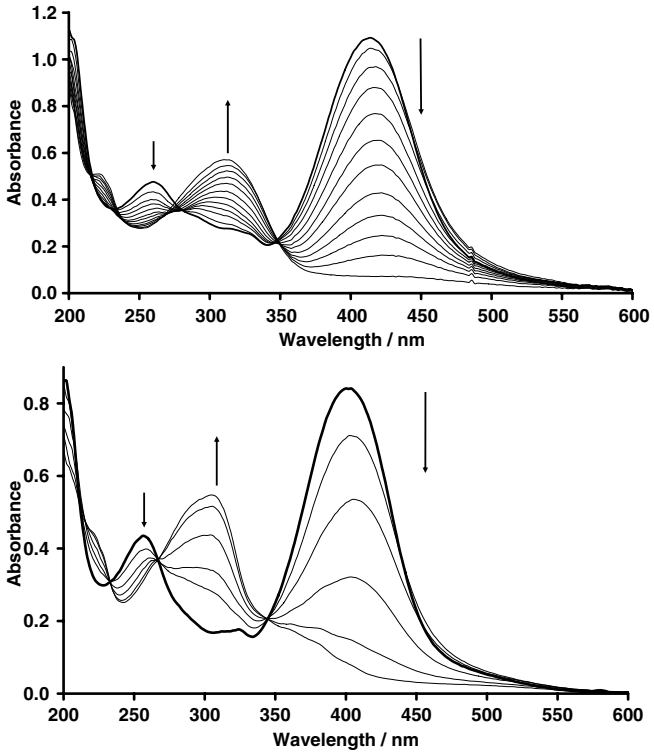

Fig. 3. Absorption behaviour of compounds **1** [2.5×10^{-5} M] (top), and **2** [2.0×10^{-5} M] (bottom) before (solid line) and after addition of CF_3SO_3H in CH_3CN. From top to bottom at 400 nm for **1**: [H^+] (M): 2.25×10^{-6}, 6.75×10^{-6}, 9.00×10^{-6}, 1.35×10^{-5}, 1.80×10^{-5}, 2.25×10^{-5}, 2.70×10^{-5}, 3.15×10^{-5}, 3.82×10^{-5}, 4.27×10^{-5}, 4.95×10^{-5} M. From top to bottom at 400 nm for **2**: [H^+] (M): 8.0×10^{-6}, 1.60×10^{-5}, 2.40×10^{-5}, 3.2×10^{-5}, 4.0×10^{-5}.

acteristic of the formation of the corresponding protonated species, the quaternarization of the amino group leading to the suppression of charge transfer within the molecule [17].

The UV–Vis absorption spectrum of compounds **1** and **2** placed in the presence of high triflate salt concentration ($\geqslant 3.0 \times 10^{-3}$ M for **1** and 3.0×10^{-2} for **2**) is thus very close to that obtained at the end of the titration by triflic acid. In particular, in both cases, the maximum wavelength of the two spectra was quite close. We propose that during the last step corresponding to addition of high concentrations of calcium triflate to compounds **1** and **2**, the related protonated species is the major species formed in solution.

Let us consider now the origin of the H^+ source: under our previous NMR experimental conditions [10], the salt to ligand ratio was below 12 equiv., and we have checked that there is no protonation reaction over a 48 h period. In contrast, under the UV–Vis conditions, the salt to ligand ratio is much higher. Consequently, the amount of impurities such as free triflic acid may increase and become a substantial source of H^+. Another explanation could be that the proton source comes from the hydrolysis of the triflate calcium salt in spectroscopic grade acetonitrile, used without subsequent dehydration. Regarding the NMR calcium titration experiments, we have performed them with dried deuterated acetonitrile and under inert atmosphere.

*2.1.4. Detection of calcium and barium perchlorate by compounds **1** and **2***

Taking into account the conclusions of the UV–Vis absorption study concerning addition of calcium triflate to ligands **1** and **2**, perchlorate salts were then preferred. They are generally used because they dissolve easily in acetonitrile and are known not to interfere with spectrophotometric measurements.

In the presence of perchlorate salts, the behaviour of dye **1** is different from that observed with the triflate salt. A representative evolution of the spectrum is displayed in Fig. 4 for calcium (top), and barium (bottom). A common feature appears for both salts: the CT band slightly decreases and progressively shifts to the red, while absorbance increases around 310 nm. It is noteworthy that no isosbestic point is observed, indicating in each case the formation of several species in solution. The variation of the absorption maximum of compound **1** (44 nm) after addition of 10^{-1} M calcium perchlorate is close to that obtained under the same conditions with the monosubstituted counterpart **4** (34 nm) [9], for which no protonation reaction occurred. These values are lower than that obtained with the related organic compound $CO(CH{=}CHC_6H_4NEt_2)_2$ (**7**) and Ca^{2+} (74 nm).

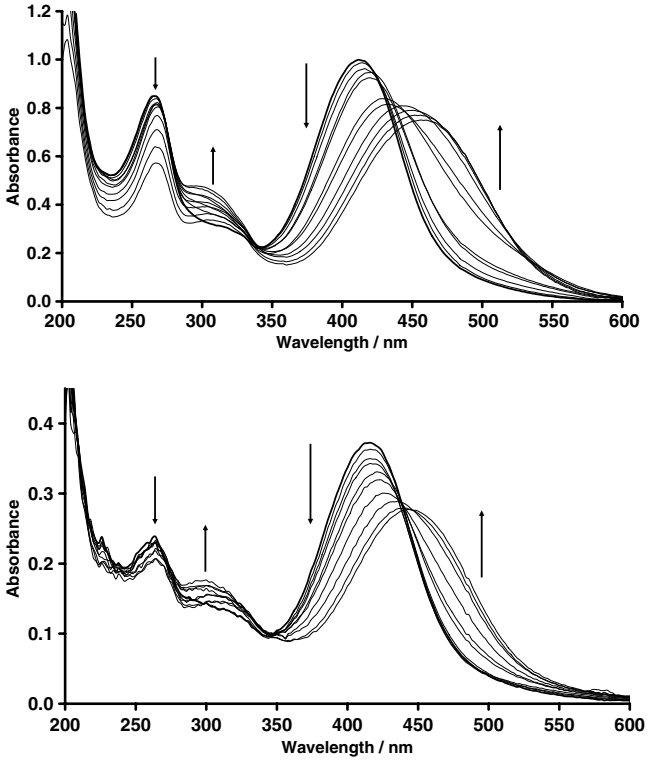

Fig. 4. Absorption behaviour of compound **1** upon addition of perchlorate salts addition, in CH_3CN; Top: **1** [2.28×10^{-5} M] (solid line), from top to bottom at 400 nm: [Ca^{2+}] (M): 1.0×10^{-5}, 2.5×10^{-4}, 7.5×10^{-4}, 1.0×10^{-3}, 2.5×10^{-3}, 1.0×10^{-2}, 2.5×10^{-2}, 5×10^{-2}, 7.5×10^{-2}, 1.0×10^{-1}. Bottom: **1** [8.50×10^{-6} M] (solid line), from top to bottom at 400 nm: [Ba^{2+}] (M): 5.0×10^{-6}, 2.5×10^{-5}, 7.5×10^{-4}, 5×10^{-3}, 1.0×10^{-2}, 2.5×10^{-2}, 5×10^{-2}, 7.5×10^{-2}, 1.0×10^{-1}.

As shown by Fig. 5, the addition of calcium or barium perchlorate salt to a solution of compound **2** leads to a behaviour quite different from that observed with compound **1**. The variation of the absorption spectrum is qualitatively similar with both salts. The intensity of the CT band decreases regularly and a new band appears at short wavelengths at 336 and 352 nm for Ca^{2+} and Ba^{2+}, respectively. No isosbestic points were detected, suggesting the formation of several L_nM_m species (where L is the ligand and M the metal cation) in equilibrium in solution. It is noteworthy that addition of perchlorate salts to solution of **1** or **2** turned the solution deep red.

The UV–Vis absorption spectra obtained with compounds **1** and **2** upon addition of the Ca^{2+} and Ba^{2+} cations clearly indicate that the main interacting sites are respectively the CO groups for **1**, and the azacrown groups for **2**. This is in perfect agreement with the thorough investigation of these interactions that we have recently performed by NMR spectroscopy [10]. However, NMR studies have revealed that the CO sites are also involved in the ligand–metal interaction for the azacrown compound **2**. The small red shift of the CT band maximum (4 and 6 nm for the Ca^{2+} and Ba^{2+} salt, respectively) observed during salt addition is probably a discrete indication of this phenomenon. From a general viewpoint, compounds **1** and **2** give a different absorption response in connection with the nature of the aza terminal groups, as previously observed for other members of this ferrocenyl chalcone family.

2.1.5. Proposition of models for the ligand–salt interactions: processing of the absorption data

To get a deeper insight into the ligand–Ca^{2+} interaction processes, we wanted to determine the number, the stoichiometry, and the association constants of the calcium adducts involved. To do so, the absorbance variation was analyzed versus cation concentration. Absorbance was recorded at three different wavelengths chosen to obtain maximum information, and the absorption spectroscopic data were processed according to the global curve-fitting method described elsewhere [14]. Figs. 6–8 are provided as chosen examples, other results are given as Supplementary Material.

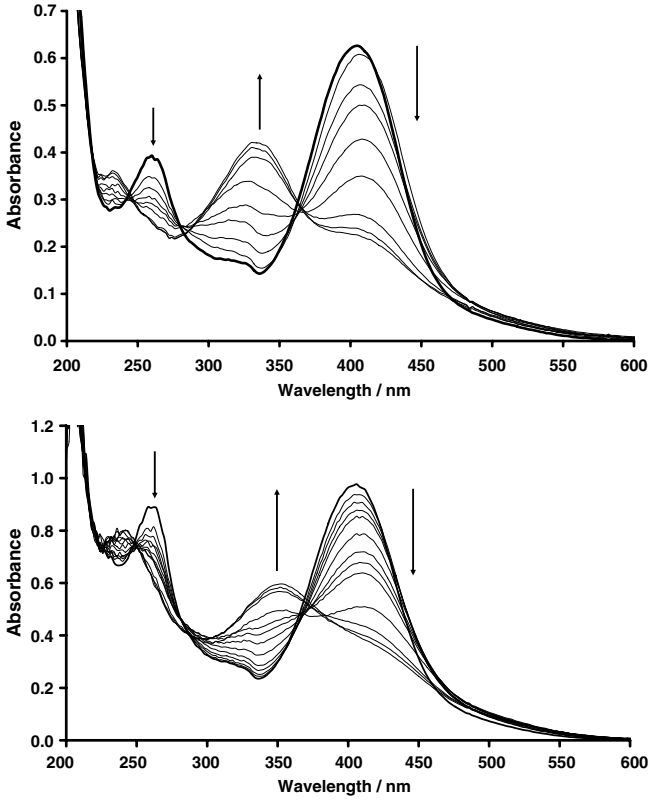

Fig. 5. Absorption behaviour of compound **2** upon addition of perchlorate salts in CH_3CN; Top: **2** [1.74×10^{-5} M] (solid line), from top to bottom at 400 nm: [Ca^{2+}] (M): 1.0×10^{-5}, 2.5×10^{-5}, 1.0×10^{-4}, 2.5×10^{-4}, 5.0×10^{-4}, 2.5×10^{-3}, 5.0×10^{-3}, 1.0×10^{-2}. Bottom: **2** [2.40×10^{-5} M] (solid line), from top to bottom at 400 nm: [Ba^{2+}] (M): 1.0×10^{-5}, 2.5×10^{-5}, 5.0×10^{-5}, 1.0×10^{-4}, 2.5×10^{-4}, 5.0×10^{-4}, 7.5×10^{-4}, 1.0×10^{-3}, 2.5×10^{-3}, 5.0×10^{-3}, 7.5×10^{-3}, 1×10^{-2}.

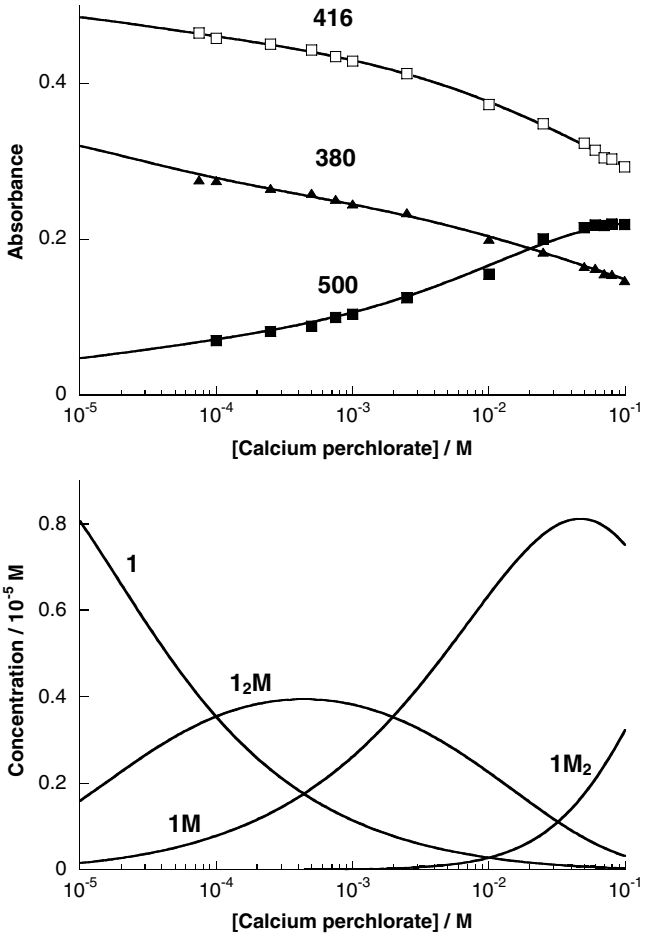

Fig. 6. Processing of the UV–Vis absorption data for compound **1** [1.14×10^{-5} M] in the presence of calcium perchlorate. (Top) Absorbance versus calcium concentration at different wavelengths in nanometers. The points are experimental and the curves (lines) were calculated by fitting the data. (Bottom) Corresponding calculated concentrations of the different species.

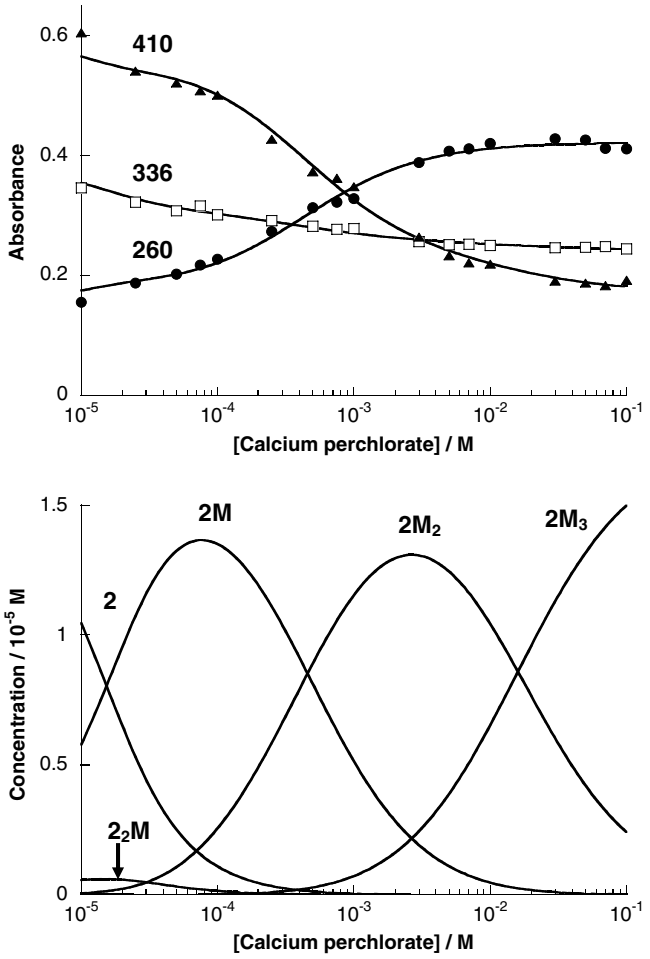

Fig. 7. Processing of the UV–Vis absorption data for compound **2** [1.74×10^{-5} M] in the presence of calcium perchlorate. (Top) Absorbance versus calcium concentration at different wavelengths in nanometers. The points are experimental and the curves (lines) were calculated by fitting the data. (Bottom) Corresponding calculated concentrations of the different species.

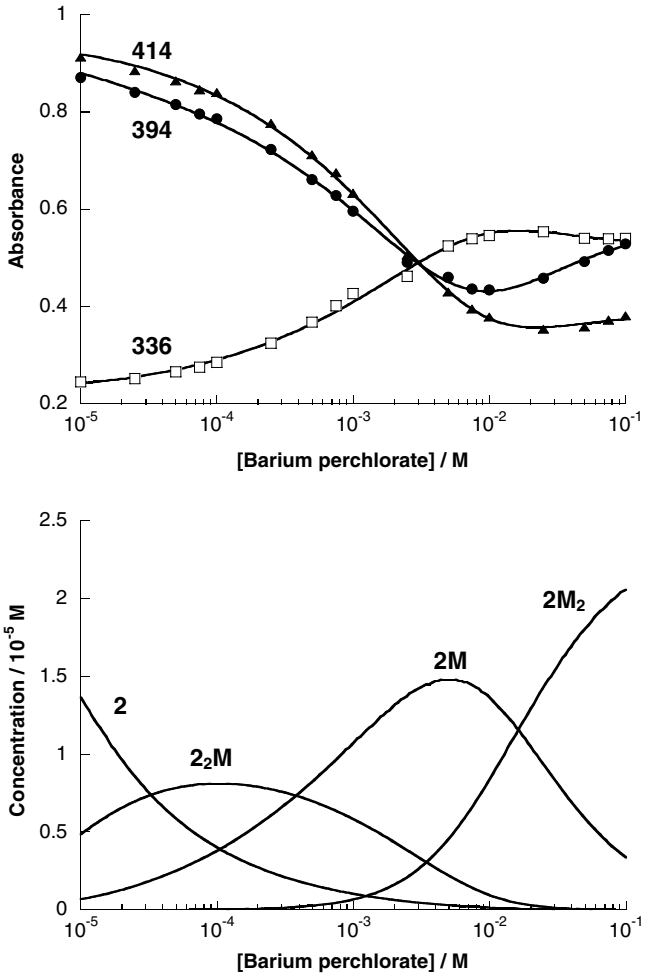

Fig. 8. Processing of the UV–Vis absorption data for compound **2** [2.4×10^{-5} M] in the presence of barium perchlorate. (Top) Absorbance vs. barium concentration at different wavelengths in nanometers. The points are experimental and the curves (lines) were calculated by fitting the data. (Bottom) Corresponding calculated concentrations of the different species.

Regarding the experiments performed with calcium triflate and ligand **1**, accurate determination of the binding constants could only be achieved for calcium concentration lower than 10^{-3} M because of the major competitive protonation reaction that takes place at high salt concentration. Except for compound **2** with calcium perchlorate, good fits were obtained by taking into account the existence of only three species of different stoichiometries: LM, L_2M and LM_2. The corresponding association constants are indicated in Table 1 (values given with a ±15% error). It is noteworthy that the association constants are nearly the same for compound **1** whatever the perchlorate salt used. For compound **2** with calcium perchlorate, considering two new L_3M and LM_3 species was necessary to get a good fit of the experimental data.

For ligand **2**, the main characteristic feature is that the highest association constants are obtained for the **2**M species with calcium perchlorate, and for the $\mathbf{2}_2$M species with barium perchlorate. The first value can be explained by the fact that the crown ring fits well the calcium ion [18]. This **2**M species is probably formed by a Ca^{2+} cation sandwiched between two crown rings of the ligand [19]. Actually, the value of the **2**M association constant is two order of magnitude higher than that obtained for the monosubstituted azacrown counterpart **5** (2.0×10^3 mol L^{-1}). This suggests that the second aza ring in **2** enhances the stability of such a **2**M adduct. In the literature, although numerous calcium-containing structures are known, only a few X-ray structures have been reported for azacrown calcium complexes [20], and unfortunately, it was not possible to obtain any X-ray structures for the **2**M species. Now, the high association constant obtained for the $\mathbf{2}_2$M species formed with barium may be explained by the fact that the bis-crown compound **2** is better suited for the complexation of calcium than for that of the bulky barium cation, and by the propensity of the Ba^{2+} cation to promote intermolecular interactions [21]. The latter point may also explain why the highest Ba^{2+} association constants is also obtained for the L_2M species with compound **1** (Table 1).

Table 1
Association constants (K_n, L mol^{-1}) related to the different species formed with ligands **1**–**2** and calcium or barium salts in acetonitrile, determined by processing the UV–Vis data (values given with ±15% error)

[Compound]	Salt	Final [salt]	[LM] K_1	[L_2M] K_2	[LM_2] K_3	[L_3M] K_4	[LM_3] K_5
[**1**]							
1.20×10^{-5}	$Ca(CF_3SO_3)_2$	3.0×10^{-3}	3.2×10^{3}	2.0×10^{6}	1.0×10^{3}		
1.14×10^{-5}	$Ca(ClO_4)_2$	1.5×10^{-1}	2.3×10^{3}	1.3×10^{6}	4.3		
8.5×10^{-6}	$Ba(ClO_4)_2$	1.0×10^{-1}	2.1×10^{4}	5.7×10^{5}	1.3×10^{1}		
[**2**]							
1.74×10^{-5}	$Ca(ClO_4)_2$	1.0×10^{-1}	1.54×10^{5}	9.03×10^{3}	2.32×10^{3}	1.93×10^{3}	6.27×10^{1}
2.4×10^{-5}	$Ba(ClO_4)_2$	1.0×10^{-1}	1.08×10^{4}	5.35×10^{5}	6.18×10^{1}		
[**2**][a]							
6.5×10^{-3}	$Ca(CF_3SO_3)_2$	6.5×10^{-2}	2.37×10^{5}	1.29×10^{2}	1.27×10^{4}	2.12×10^{3}	2.89×10^{1}

[a] Related to compound **2** with calcium triflate and determined by processing the NMR data, see Ref. [10].

We have verified that the set of values obtained by fitting the UV–Vis absorption data of **2** with calcium perchlorate provides a good fit of the UV–Vis data obtained with this compound and calcium triflate until a 2.5×10^{-3} M salt concentration. This confirms that, in this restricted range of calcium salt concentration, the absorption response of ligand **2** is not sensitive to the nature of the calcium salt used (perchlorate or triflate), as it was the case for its monosubstituted counterpart **5**.

Interestingly, the set of association constants issued from processing the UV–Vis data of **2** with calcium perchlorate is also very close to that obtained from ^{1}H NMR data with calcium triflate (Table 1). Compound **2** thus provides here a rare opportunity to fit the data obtained by both techniques with nearly the same set of association constants. To our knowledge, such an opportunity was only provided until now by the monosubstituted counterpart **5** when considering its ^{13}C NMR and UV–Vis absorption data [9]. In this family of ferrocenyl chalcones, this trend seems to be a specificity of the azacrown derivatives when compared to the N-alkyl compounds.

In other respects, mass spectra were recorded with samples of compounds **2** (5×10^{-3} M) containing different equivalents of calcium perchlorate, and the LM_m major species were detected; similarly, the measurements realized with calcium triflate have revealed all the peaks corresponding to the species expected, thus providing thus strong support for their existence in solution [10].

2.2. Fluorescence study

2.2.1. Detection of calcium and barium perchlorate by fluorescent compound *1*

Few examples of ferrocenyl fluorescent ion sensors have been described, probably because ferrocene is known to be an efficient fluorescence quencher [22]. In the literature very few ferrocenyl derivatives have a satisfying fluorescence efficiency. Compound **1** was designed to possess this original property and we have previously shown that it could behave as a fluorescent probe, providing a different and noticeable response over a wide range of calcium triflate concentrations [16b]. To complete our study, we have examined here the capability of compound **1** to detect calcium and barium perchlorates by fluorescence spectroscopy.

In the absence of salts, the emission spectrum of **1** in acetonitrile displayed only one emission band with a maximum at 560 nm, independently of the excitation wavelength. In the presence of calcium perchlorate, **1** (3.5×10^{-6} M) was excited at $\lambda = 338$ nm to minimize the effects of absorption variations. Fig. 9 (top) shows that a two-step behaviour is observed: First the intensity increases until the Ca^{2+} concentration reaches 10 equiv. (arrow a), then it decreases slowly. Two main differences are noted by comparison with the calcium triflate titration experiments. In the present case, total fluorescence quenching is not observed, even for a 10^{-1} M salt concentration, and the emission maximum is subsequently red-shifted by 24 nm. The latter observation could be explained by the fact that the CO groups of the molecules are involved in the interaction processes that take place in the excited state. The variations of the fluorescence spectrum cannot be justified by the disappearance of the emissive ligand and the formation of a unique species. It seems that several species contribute to fluorescence emission. Actually, the set of association constants obtained by processing the UV–Vis absorption data of **1** and calcium perchlorate was used to process the fluorescence data, and a good fit was obtained. However, caution is required because we have no information about the deactivation process that the different species may undergo in the excited state.

With barium perchlorate (Fig. 9, bottom) the same general trends as for calcium perchlorate are obtained. The maximum fluorescence intensity is reached with 2 equiv. of salt, the bathochromic shift of the emission maximum is 14 nm, and processing the emission data according to the previous method shows that the species detected by absorption spectroscopy could also be involved in the fluorescence process. In this case, the enhancement of the fluorescence intensity at low salt concentration could be connected with the formation of the $\mathbf{1}_2$M species which would enhance the rigidity of the system, thus limiting

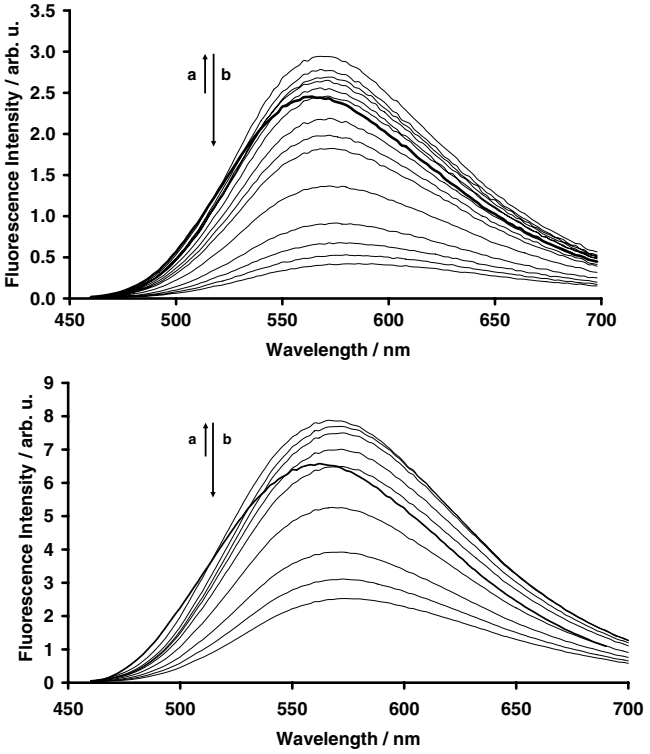

Fig. 9. Fluorescence behaviour of compound **1** upon perchlorate salts addition in CH_3CN; Top: **1** [3.5×10^{-6} M] (solid line), from top to bottom: [Ca^{2+}] (M): 2.5×10^{-5}, 1.0×10^{-5}, 1.0×10^{-4}, 2.5×10^{-6}, 1.5×10^{-6}, 0.0, 2.5×10^{-3}, 5×10^{-3}, 7.5×10^{-3}, 1.0×10^{-2}, 2.0×10^{-2}, 4.0×10^{-2}, 6.0×10^{-2}, 8.0×10^{-2}, 1.0×10^{-1}, $\lambda_{ex}=338$ nm. Bottom: **1** 1.9×10^{-6} M (solid line), from top to bottom: [Ba^{2+}] (M): 2.5×10^{-6}, 2.5×10^{-5}, 1.0×10^{-4}, 7.5×10^{-4}, 0.0, 1.0×10^{-2}, 2.5×10^{-2}, 5.0×10^{-2}, 7.5×10^{-2}, 1.0×10^{-1}, $\lambda_{ex}=440$ nm.

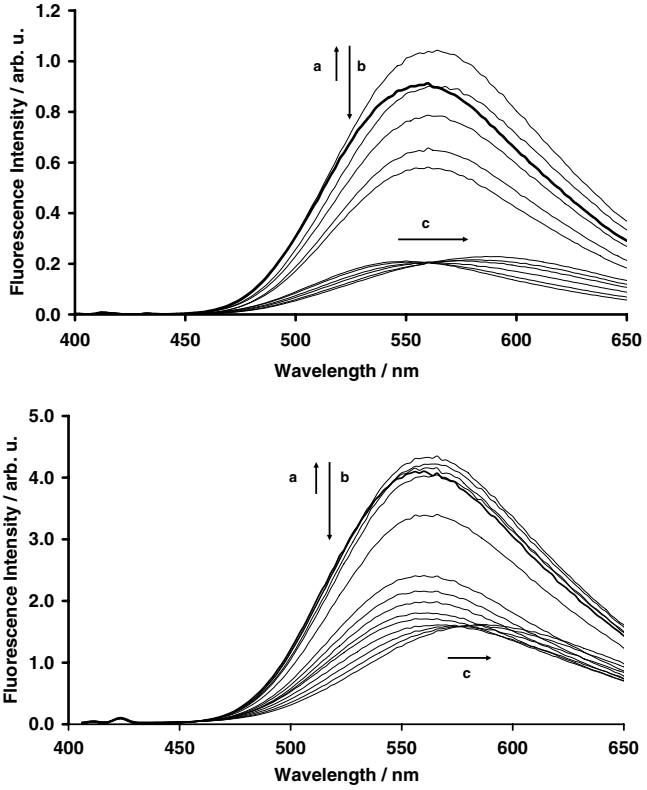

Fig. 10. Fluorescence behaviour of compound **2** upon perchlorate salts addition in CH_3CN; Top: **2** [3.3×10^{-6} M] (solid line), from top to bottom: [Ca^{2+}] (M): 5.0×10^{-6}, 0.0, 2.5×10^{-5}, 5.0×10^{-5}, 1.0×10^{-4}, 5.0×10^{-4}, 5×10^{-3}, 1.0×10^{-2}, 2.0×10^{-2}, 4.0×10^{-2}, 6.0×10^{-2}, 1.0×10^{-1}, $\lambda_{ex}=366$ nm. Bottom: **2** [2.55×10^{-6} M] (solid line), from top to bottom: [Ba^{2+}] (M): 1.0×10^{-5}, 2.5×10^{-5}, 2.5×10^{-6}, 0.0, 7.5×10^{-5}, 1.0×10^{-4}, 2.5×10^{-4}, 2.5×10^{-3}, 5×10^{-3}, 7.5×10^{-3}, 1.0×10^{-2}, 2.5×10^{-2}, 5.0×10^{-2}, 7.5×10^{-2}, 1.0×10^{-1}, $\lambda_{ex}=368$ nm.

the non-radiative deactivation processes due to the vibration modes of the molecule.

2.2.2. Detection of calcium and barium perchlorate by fluorescent compound 2

Interestingly, compound **2** is also fluorescent and exhibits the same emission characteristics as compound **1** in acetonitrile. In this solvent, the quantum yield of **2** is up to 7.6×10^{-2}. This value is close to that obtained for compound **1** (7.7×10^{-2}) and related organic compounds [14b]. Consequently, substituting the NEt_2 groups by the azacrown groups in the molecular framework of **1** retains the fluorescence properties.

In the presence of calcium perchlorate, compound **2** (2.6×10^{-6} M) was excited at $\lambda=366$ nm. The emission spectrum is strongly perturbed by subsequent additions of salt (Fig. 10, top). A three-step behaviour is now observed: first the intensity increases until the Ca^{2+} concentration reaches 10 equiv. (arrow a) and a concomitant bathochromic shift (4 nm) of the maximum emission wavelength is observed, suggesting possible CO interactions processes with the cation. Then, the intensity decreases stepwise, accompanying a hypsochromic shift of the emission maximum (10 nm with respect to the spectrum of the free ligand) (arrow b). Finally, when a 10^{-2} M salt concentration is reached, a significant bathochromic shift (40 nm) of the emission maximum occurs (arrow c). During this third step an isoemissive point is located at 560 nm.

The first step is reminiscent of that obtained for ligand **1** and calcium perchlorate. The second step is more representative of the nature of ligand **2**: the hypsochromic shift observed could be attributed to an interaction of the azacrown with Ca^{2+}, leading to the formation of one or several species that emit at short wavelengths. Finally, the third step is characteristic of the formation of new species that emit at higher wavelengths.

In the presence of barium perchlorate (Fig. 10, bottom), compound **2** exhibits the same general fluorescence trends. The emission maximum undergoes a shift that is successively bathochromic (accompanying the fluorescence enhancement indicated by arrow a), hypsochromic (accompanying the fluorescence decrease indicated by arrow b), and bathochromic again. The corresponding shift values are respectively 6, 4, and 30 nm. In agreement with NMR and UV–Vis absorption data, these variations reflect the possibility of interactions between the cation and the CO or azacrown groups of **2**.

In the literature, non-monotonous variations of the fluorescence intensity are rarely reported for ligand–ion interactions. Interestingly, Otsuki et al. have reported a two-step variation for a diether-crown compound [23]. During cesium titration, a decrease of the fluorescence intensity of the ligand is observed at low cation concentration, whereas an increase is observed at high cation concentration. This change has been explained by the existence of an equilibrium between two species, the first one being a sandwich LM complex, and the second one an LM_2 type complex. The fluorescence intensity variation has been attributed to conformational change of the ligand when passing from the first adduct to the second one. In our case, the fluorescence behaviour of ligand **2** is more likely to result from the presence of several interacting sites, although conformational changes may also take place.

Regarding now the variation of the spectrum position, the first bathochromic shift could be attributed to the interaction of the cation with only one crown. A link can be made with the bathochromic shift of 28 nm of the emission spectrum that has been reported for bis-crown compound [CO(CH=CHC$_6$H$_4$-*p*-aza-15-crown-5)$_2$] in the presence of calcium perchlorate [14b]. This unsymmetrical molecule formed by complexation of only one crown would emit at higher wavelengths than the symmetrical one. Nevertheless, this molecule is not strictly comparable to ours. Hypsochromic shifts could correspond to an interaction where both crowns are involved. The final bathochromic shift can be attributed to interaction of the carbonyl group with the cation, or with water molecules brought by the hydrated perchlorate salt. The overall variations of the initial wavelength could in fact be due to a combination of all these phenomena. Finally, the isoemissive point observed at high salt concentration may correspond to a simple equilibrium between two emissive species [24].

To sum up, the variations of the fluorescence spectrum reflect the existence of several interactions in solution involving the azacrown and CO groups of the excited molecules. For compound **2**, the hypsochromic shift of the wavelength constitutes the signature of the azacrown ligand when compared to compound **1**. According to the previous study, at very high calcium concentration, the final emissive species obtained could be the LM_3 species.

As for compound **1**, the fluorescence data obtained with compound **2** in the presence of Ca^{2+} and Ba^{2+} perchlorate were processed with our global curve-fitting method, using the set of species and association constants already calculated for the ground state. No satisfying fits were attained in these conditions for the calcium salt. In particular, the L_nCa^{2+} species were not necessary to fit the data. This result suggests that, with the calcium salt, an equilibrium different from that of the ground state is reached in the excited state. In contrast, a correct fit was achieved with the barium cation, indicating that the equilibrium present in the ground state could be similar to that of the excited state. This could indicate that, with Ba^{2+}, the final emissive species is the LM_2 species.

*2.2.3. Triflate cation detection tests: **2** and the lithium cation*

Before developing the fluorescence detection study with the calcium and barium perchlorate salts, compounds **1** and **2** have been evaluated towards other triflate cations (Li^+, Na^+, K^+, Mg^{2+}, Ca^{2+}, Ba^{2+}, Zn^{2+}, and Cu^{2+}). Each ligand has been excited at the wavelength of a quasi-isosbestic point. This one was determined by UV–Vis absorption study by taking the spectrum of the ligand in the presence of four different salt concentrations ranging from 10^{-4} M to 10^{-3} M. Adding a solution of salt [10^{-3} M] on compound **1** [3×10^{-6} M] induces a red shift (5–8 nm) of the maximum emission wavelength, with a partial or total decrease of the fluorescence intensity. Under the same conditions, a blue shift is systematically observed with compound **2**, whereas the fluorescence intensity decreases, except for the sodium and the lithium cations (see Fig. 11). Under these concentrations, the fluorescence is totally quenched by Cu^{2+} for **1** and also by Cs^{2+} and Hg^{2+} for **2**. For the Cu^{2+} cation this is probably due to an electron transfer process from the excited molecule to the cation leading to non-radiative deactivation processes and to fluorescence quenching [25]. Interestingly, the strongest hypsochromic shift ($\Delta\lambda = 12$ nm) and enhancement of the fluorescence intensity (25%) are observed with the Li^+ cation. Owing to the known biological interest for this cation [26], and the fact that chemical separation and enrichment processes of isotopes of this cation using azacrown derivatives exist [27], we have undertaken a rapid study about this cation. NMR investigations show that weak interaction probably takes place with the crown ring inducing a 0.38 ppm downfield-shift and a broadening of the ^{7}Li signal when compared to that of Li(CF_3SO_3) salt ($\delta = -2.48$ ppm). This crown interaction is in agreement with data reported for the [(C_5H_5)Fe(C_5H_4CO-aza-15-crown-5)] compound but not with the [Fe(C_5H_4CO-aza-15-crown-5)$_2$] compound where a CO interaction is preferred [28]. The Li^+ cation is small and different coordination modes involving all, or a part of the nitrogen or/and

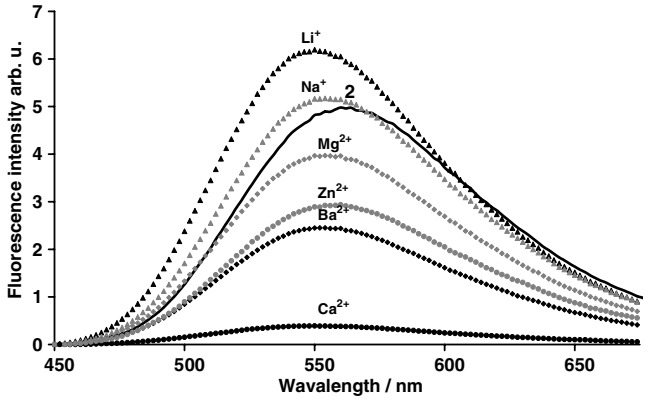

Fig. 11. Fluorescence behaviour of compound **2** [3.0×10^{-6} M] in the absence (solid line), and upon addition of selected triflate salts [10^{-3} M] in CH_3CN. From top to bottom, λ_{ex}: 360, 356, 368, 354, 366, 342, 368, 366 nm.

oxygen atoms of the crown can be envisaged [29]. However, compound **2** allows an optical UV–Vis lithium detection: a decrease of the CT band at 404 nm is observed, while a new band grows up at 280 nm. Again, this result strengthens the NMR results, indicating that the main interaction sites are probably the azacrown rings. Till now, the hyperchromic effect observed by fluorescence spectroscopy remains unexplained. Mass data indicate that the four LM, LM_2, LM_3, and L_2M species could be involved here, with peaks observed at 887 $[LM]^+$, 1043 $[LM_2X]^{2+}$ and 447 $[LM_2]^{2+}$, 1199 $[LM_3X_2]^+$, and 1768 $[L_2M]^+$. However, in contrast with Grossel's compound [28], **2** does not electrochemically detect Li^+. For this reason we have not developed further the optical analysis, as we were first interested by multi-detection of the same cation by different techniques.

3. Concluding remarks

With respect to the work already published on this family of ferrocenyl chalcones, the present study brings interesting highlights on the three following points.

(i) We have recently shown that ferrocenyl chalcones **1** and **2** are good electrochemical calcium sensors, and "non-classical" electrochemical barium sensors, the detection pathway being different according to the cation considered. In this work, we show that both compounds detect calcium and barium cations in a similar manner. The variations of the absorption spectrum depend on the nature of the ligand and, consequently, on the interacting sites involved in the ligand–cation interaction. The main interacting sites are the CO groups and the azacrown rings for **1** and **2**, respectively. We give evidence that each ligand–cation interaction is complex and involves several L_nM_m species. This is in total agreement with previously reported NMR and mass spectrometry analyses.

(ii) This study also highlights that, under UV–Vis absorption conditions, the azacrown compound **2** is less sensitive to the nature of the calcium source (triflate or perchorate) than its NEt_2 counterpart **1**. Actually, whatever the salt used, the same absorption spectrum is obtained until salt concentration reaches 2.5×10^{-3} M. The same set of association constants can be used to fit these data, showing that the same species are involved with both salts. Remembering the results obtained with the monosubstituted counterparts, this fact points out that the azacrown derivatives have a better chemical stability towards calcium triflate than their amino alkyl counterparts.

(iii) Compounds **1** and **2** exhibit good fluorescence efficiency in acetonitrile. In this medium, they can detect several cations by fluorimetry. Using calcium and barium perchlorate salts, we illustrate that a complex and unusual fluorescence detection behaviour may occur for ferrocenyl chalcone derivatives. Nevertheless, non-monotonous variations of the fluorescence response reduce the interest of these ligands for use as fluorescent probes.

These ferrocenyl chalcones can give varied physicochemical responses upon addition of a given cation (Ca^{2+} or Ba^{2+}), and can be sensitive to the nature of the associated anion. Regarding electrochemistry, this last property constantly appears with calcium salt whatever the ligand used. Considering now UV–Vis spectroscopy, the sensitivity to anion nature depends on the nature of the ligand used and can be modulated by the calcium salt concentration. These ligands are good (and original) electrochemical and UV–Vis optical calcium and barium sensors, and consequently constitute intriguing examples of multi-channel cation chemosensors with unprecedented fluorescence detection behaviour.

4. Experimental

4.1. Materials

Spectroscopic grade acetonitrile (Merck) was used for absorption measurements. HCF_3SO_3 (98%) was from Aldrich. Calcium salts: $Ca(CF_3SO_3)_2$ (96%) and $Ca(ClO_4)_2 \cdot 4H_2O$ (99%) were from Strem and Aldrich, respectively. $Ba(ClO_4)_2$ (99.9%) was from Aldrich. Other salts: $LiCF_3SO_3$ (99%) (Strem), $NaCF_3SO_3$ (97%), KCF_3SO_3 (99%) (Acros), $Mg(CF_3SO_3)_2$ (98%) (Fluka), $Cu(CF_3SO_3)_2$ (98%), $Zn(CF_3SO_3)_2$ (98%) (Aldrich), $Cs(CF_3SO_3)_2$ (98%) (Strem), $Hg(CF_3SO_3)_2$ (98%) (Strem). Triflate salts were dried, weighed, and dissolved in acetonitrile solutions of ligands under inert atmosphere before use of the mixtures. Warning! Perchlorate salts are hazardous because of the possibility of explosion! Compounds **1** and **2** were prepared according to our published procedures [10].

4.2. General instrumentation and procedures

The solutions of compounds **1** and **2** were light-protected before each measurement. Mass spectra were obtained at the Service Commun de Spectrométrie de Masse de l'Université Paul Sabatier et du CNRS de Toulouse. Spectra were performed on a triple quadrupole mass spectrometer (Perkin–Elmer Sciex API 365) using electrospray as the ionization mode (positive mode). The infusion rate was 5 μL/min.

4.3. Optical measurements

4.3.1. Apparatus

UV–Vis absorption spectra were recorded on a Hewlett–Packard 8452 A diode array spectrophotometer. It was checked that the absorption spectra did not vary over a period of 2 h. Cells of 1 cm optical path-length were used. Steady-state fluorescence work was performed on a Photon Technology International (PTI) Quanta Master 1

spectrofluorometer. All fluorescence spectra were corrected. The fluorescence quantum yield was determined relative to coumarin 6 in ethanol as the standard ($\Phi_F = 0.78$) [30]. The measurements were conducted at 20 °C in a thermostated cell-holder.

4.3.2. Data analysis

All the simulations and parametric adjustments were performed using home-made software, SA version 3, as described in Refs. [14,9]. Absorbance A was related to the concentration C_i using Beer–Lambert's law: $A = l\sum(\varepsilon_i C_i)$ were ε_i is the molar absorption coefficient of the species i and l is the optical path length. The system of the equilibrium equations with independent variables was numerically solved by an iterative method. The sum of the squares of the differences between the experimental values and those of the numerical calculation was minimized by a Powell nonlinear minimization algorithm.

Acknowledgements

This work was supported by the CNRS and the French Ministry of Research (doctoral fellowship to J.M.).

Appendix A. Supporting material

Supplementary data associated with this article can be found, in the online version, at doi:10.1016/j.jorganchem.2007.03.044.

References

[1] (a) P.D. Beer, F. Szemes, V. Balzani, C. M Salà, M.G. B Drew, S.W. Dent, M. Maestri, J. Am. Chem. Soc. 119 (1997) 11864–11875;
(b) P.D. Beer, J. Cadman, Coord. Chem. Rev. 205 (2000) 131–155;
(c) F. Sancenon, A. Benito, F.J. Hernandez, J. M Lloris, R. Martinez-Manez, T. Pardo, J. Soto, Eur. J. Inorg. Chem. (2002) 866–875;
(d) L.-J. Kuo, J.-H. Liao, C.-T. Chen, C.-H. Huang, C.-H. Chen, J.-M. Fang, Org. Lett. 5 (2003) 1821–1824;
(e) F. Oton, A. Tarraga, M.D. Velasco, A. Espinosa, P. Molina, Chem. Commun. (2004) 1658–1659;
(f) A. Caballero, R. Tormos, A. Espinosa, M.D. Velasco, A. Tarraga, M.A. Miranda, P. Molina, Org. Lett. (2004) 4599–4602;
(g) D. Jimenez, R. Martinez-Manez, F. Sancenon, J.V. Ros-Lis, J. Soto, A. Benito, E. Garcia-Breijo, Eur. J. Inorg. Chem. (2005) 2393–2403.

[2] (a) P.D. Harvey, L. Gan, C. Aubry, Can J. Chem. 68 (1990) 2278–2288;
(b) P.D. Harvey, L. Gan, Inorg. Chem. 30 (1991) 3239–3241;
(c) L. Cuffe, R.D.A. Hudson, J.F. Gallagher, S. Jennings, C.J. McAdam, R.B.T. Connelly, A.R. Manning, B.H. Robinson, J. Simpson, Organometallics 24 (2005) 2051–2060;
(d) E.M. McGale, B.H. Robinson, J. Simpson, Organometallics 22 (2003) 931–939;
(e) C.J. McAdam, J.L. Morgan, B.H. Robinson, J. Simpson, Organometallics 22 (2003) 5126–5136.

[3] R. Martinez, I. Ratera, A. Tarraga, P. Molina, J. Veciana, Chem. Commun. (2006) 3809–3811.

[4] (a) D.C. Magri, G.J. Brown, G.D. McClean, A.P. de Silva, J. Am. Chem. Soc. 128 (2006) 4950–4951;
(b) M.N. Chatterjee, E.R. Kay, D.A. Leigh, J. Am. Chem. Soc. 128 (2006) 4058–4073;
(c) V. Amendolla, L. Fabrizzi, F. Foti, M. Licchelli, C. Mangano, P. Pallavicini, A. Poggi, D. Sacchi, A. Taglietti, Coord. Chem. Rev. 250 (2006) 273–299;
(d) C. Triefninger, H. Röhr, K. Rurack, J. Daub, Angew. Chem., Int. Ed. 44 (2005) 6943–6947.

[5] (a) For examples: X. Wu, E.R.T. Tieking, I. Kostetski, N. Kocherginsky, A.L.C. Tan, S.B. Khoo, P. Vilairat, M.-L. Go, Eur. J. Pharm. Sci. 27 (2006) 175–187;
(b) S.-J. Ji, Z.L. Shen, D.-G. Gu, S.Y. Wang, J. Organomet. Chem. 689 (2004) 1843–1848;
(c) A. Ferle-Vidovic, M. Poljak-Blazi, V. Rapic, D. Skare, Cancer Biother. Radio. 15 (2000) 617–624;
(d) M. Prokesova, E. Solcaniova, S. Toma, K.W. Muir, A.A. Torabi, G. Knox, J. Org. Chem. 61 (1996) 3392–3397;
(e) D. Villemin, B. Martin, M. Puciova, S. Toma, J. Organomet. Chem. 484 (1994) 27–31;
(f) A.G. Nagy, P. Sohar, J. Marton, J. Organomet. Chem. 410 (1991) 357–364;
(g) A.G. Nagy, S. Toma, J. Organomet. Chem. 266 (1984) 257–268;
(h) A.M. El-Khawaga, K.M. Hassan, A.A. Khalaf, Z. Naturforsch. 36b (1981) 119–122;
(i) A.N. Nesmeyanov, G.B. Shulp'in, L.V. Rybin, N.T. Gubenko, M.I. Rybinskaya, P.V. Petrovkii, V.I. Robas, J. Gener. Chem. USSR 44 (1974) 1994–2001;
(j) S. Stankoviansky, A. Beno, S. Toma, E. Gono, Chem. Zvesti 24 (1970) 19–27;
(k) S. Toma, A. Perjessy, Chem. Zvesti 23 (1969) 343–351;
(l) J.P.C.G. Dubosc, US Patent 3 (1967) 335,008;
(m) M. Furdik, S. Toma, Chem. Zvesti 20 (1966) 326–335;
(n) J. Boichard, J.P. Monin, J. Tirouflet, Bull. Soc. Chim. Fr. 4 (1963) 851–856;
(o) T.A. Mashburn Jr., C.E. Cain, C.R. Hauser, J. Org. Chem. 25 (1960) 1982–1986.

[6] (a) B. Delavaux-Nicot, S. Fery-Forgues, Eur. J. Inorg. Chem. (1999) 1821–1825;
(b) S. Fery-Forgues, B. Delavaux-Nicot, J. Photochem. Photobiol. A Chem. 132 (2000) 137–159.

[7] B. Delavaux-Nicot, J. Maynadié, D. Lavabre, S. Fery-Forgues, Inorg. Chem. 45 (2006) 5691–5702.

[8] (a) B. Delavaux-Nicot, J. Maynadié, D. Lavabre, C. Lepetit, B. Donnadieu, Eur. J. Inorg. Chem. (2005) 2493–2505;
(b) J. Maynadié, B. Delavaux-Nicot, D. Lavabre, B. Donnadieu, J.C. Daran, A. Sournia-Saquet, Inorg. Chem. 43 (2004) 2064–2077.

[9] J. Maynadié, B. Delavaux-Nicot, D. Lavabre, S. Fery-Forgues, J. Organomet. Chem. 691 (2006) 1101–1109.

[10] B. Delavaux-Nicot, J. Maynadié, D. Lavabre, S. Fery-Forgues, J. Organomet. Chem. 692 (2007) 874–886.

[11] (a) M.V. Barnabas, A. Liu, A.D. Trifuniac, V.V. Krongauz, C.T. Chang, J. Phys. Chem. 96 (1992) 212–217;
(b) R.M. Silverstein, G.C. Bassler, T.C. Moril, in: Spectroscopic Identification of Organic Compounds, fourth ed., John Wiley & Sons, New York, 1981, p. 316 (Chapter VI).

[12] (a) J.A. Mata, E. Péris, R. Llusar, S. Uriel, M.P. Cifuentes, M.G. Humphrey, M. Samoc, B. Luther-Davies, Eur. J. Inorg. Chem. (2001) 2113–2122;
(b) W.-Y. Wong, G.-L. Lu, C.K. Wong, K.-H. Choi, J. Organomet. Chem. 637 (2001) 159–166;
(c) S. Sakanishi, D.A. Bardwell, S. Couchman, J.C. Jeffery, J.A. McCleverty, M.D. Ward, J. Organomet. Chem. 528 (1997) 35–45;
(d) M.S. Soliman, A.A. Khalaf, S.T. Ezmirly, O. Abdel-Hafez, Can. J. Spectrosc. 34 (1989) 146–151;
(e) S. Toma, A. Gaplovsky, I. Pavlik, Monatsh. Chem. 116 (1985) 479–486;
(f) Y.S. Sohn, D.N. Hendrickson, H.B. Gray, J. Am. Chem. Soc. 93 (1971) 3603–3620.

[13] (a) K.R. Thomas, J.T. Lin, J. Organomet. Chem. 63 (2001) 139–144;
(b) K.R. Thomas, J.T. Lin, Y.S. Wen, Organometallics 19 (2000) 1008–1012.

[14] (a) S. Fery-Forgues, D. Lavabre, D. Rochal, New J. Chem. 22 (1998) 1531–1538;
(b) N. Marcotte, S. Fery-Forgues, D. Lavabre, S. Marguet, V.G. Pivovarenko, J. Phys. Chem. A 103 (1999) 3163–3170.
[15] (a) K. Rurack, W. Rettig, U. Resh-Genger, Chem. Commun. (2000) 407–408;
(b) M. Kollmannsberfer, K. Rurack, U. Resh-Genger, J. Daub, J. Phys. Chem. A 102 (1998) 10211–10220;
(c) S. Fery-Forgues, M.-T. Le Bris, J.-P. Guetté, B. Valeur, J. Phys. Chem. 92 (1998) 6233–6237;
(d) H. Mrozek, H. Nikol, A. Vogler, F. Vögtle, J. Photochem. Photobiol. A. Chem. 84 (1994) 227–231.
[16] (a) T. Ukai, H. Kawazura, Y. Ishii, J.J. Bonnet, J.A. Ibers, J. Organomet. Chem. 65 (1974) 253–266;
(b) J. Maynadié, B. Delavaux-Nicot, S. Fery-Forgues, D. Lavabre, R. Mathieu, Inorg. Chem. 41 (2002) 5002–5004.
[17] L. Antonov, N. Mateeva, M. Mitewa, St. Stoyanov, Dyes Pigments 30 (1996) 235–243.
[18] (a) C.J. Pedersen, H.K. Frendsdorff, Angew. Chem., Int. Ed. Engl. 11 (1972) 16–25;
(b) B. Dietrich, J. Chem. Educ. 62 (1985) 954–964.
[19] T. Akutagawa, N. Takamatsu, K. Shitagami, T. Hasegawa, T. Nakamura, T. Inabe, W. Fujita, K. Awaga, J. Mater. Chem. 11 (2001) 2118–2124.
[20] (a) S. Itoh, H. Kumey, S. Nagatomo, T. Kitagawa, S. Fukuzumi, J. Am. Chem. Soc. 123 (2001) 2165–2175;
(b) D. Hall, A. Leineweber, J.H.R. Tucker, D. Williams, J. Organomet. Chem. 523 (1996) 13–22;
(c) J. Hu, L.J. Barbour, R. Ferdani, G.W. Gokel, J. Chem. Commun. (2002) 1806–1807.
[21] F. Vögtle, Supramolecular Chemistry, Wiley, New York, 1991.
[22] G.L. Geoffroy, M.S. Wrighton, Organometallic Photochemistry, Academic Press, New York, 1979, pp. 230–257 (Chapter 5).
[23] J. Otsuki, T. Yamagata, K. Ohmuro, K. Araki, T. Takido, M. Seno, Bull. Chem. Soc. Jpn. 74 (2001) 333–337.
[24] (a) P. Crochet, J.-P. Malval, R. Lapouyade, Chem. Commun. (2000) 289–290;
(b) K. Rurack, U. Resch-Genger, J.-L. Bricks, M. Spieles, Chem. Commun. (2000) 2103–2104;
(c) J.-P. Malval, C. Chaimbault, B. Fischer, J.-P. Morand, R. Lapouyade, Res. Chem. Intermediat. 27 (2001) 21–34.
[25] B. Valeur, I. Leray, Coord. Chem. Rev. 205 (2000) 3–40.
[26] (a) U. Schiemann, K. Hengst, J. Affect. Disorders 70 (2002) 85–90;
(b) A. El. Khoury, L. Jonhson, A. Aberg-Wistedt, R. Stain-Malmgren, Psychiatr. Res. 105 (2001) 33–44;
(c) M.L. Bourgeois, Ann. Med. Psychol. 159 (2001) 251–260;
(d) R.S.B. Williams, A.J. Hardwood, Trends Pharmacol. Sci. 21 (2000) 61–64.
[27] (a) K. Wilcox, G.E. Pacey, Talanta 38 (1991) 1315–1324;
(b) D.W. Kim, C.P. Hong, C.S. Kim, Y.K. Jeong, J.K. Lee, J. Radioanal. Nucl. Chem. 220 (1997) 229–231;
(c) D.W. Kim, Y. Chung, K.Y. Choi, Y.-I. Lee, Y.K. Jeong, Y.H. Jang, Anal. Sci. Technol. 10 (1997) 403–407;
(d) D.W. Kim, B.-K. Jeon, B.-M. Kang, K.Y. Choi, H.-I. Ryu, Main Group Met. Chem. 24 (2001) 751–755.
[28] M.C. Grossel, D.G. Hamilton, J.I. Fuller, E. Millan-Barios, J. Chem. Soc., Dalton. Trans. (1997) 3471–3477.
[29] (a) T.M. Barclay, A. McAuley, S. Subramanian, Chem. Commun. (2002) 170–171;
(b) C.A. Reiss, K. Goubitz, D. Heijdenrijk, Acta Crystallogr. C 46 (1990) 465–467.
[30] G.A. Reynolds, K.H. Drexhage, Opt. Commun. 13 (1975) 222–225.